European Polymer Journal 44 (2008) 1996–2004

Contents lists available at ScienceDirect

European Polymer Journal

journal homepage: www.elsevier.com/locate/europolj

Macromolecular Nanotechnology

Water-induced (nano) organization in poly(ethyl acrylate-*co*-hydroxyethyl acrylate) networks

Alberto J. Campillo-Fernández [a], Manuel Salmerón Sánchez [a,b,c,*], Roser Sabater i Serra [a], José María Meseguer Dueñas [a], Manuel Monleón Pradas [a,b,c], José Luis Gómez Ribelles [a,b,c]

[a] Center for Biomaterials, Universidad Politécnica de Valencia, 46022 Valencia, Spain
[b] Centro de Investigación Príncipe Felipe, Autopista del Saler 16, 46013 Valencia, Spain
[c] CIBER en Bioingeniería, Biomateriales y Nanomedicina, Valencia, Spain

ARTICLE INFO

Article history:
Received 26 September 2007
Received in revised form 9 April 2008
Accepted 18 April 2008
Available online 27 April 2008

Keywords:
Hydrogel
Copolymer networks
Nanoheterogenity
Hydrophobic effect

ABSTRACT

The conformational changes in poly(ethyl acrylate-*co*-hydroxyethyl acrylate), P(EA-*co*-HEA) chains, which constitute a copolymer network hydrogel, induced by the presence of water are investigated by different experimental techniques and compared with the behaviour of the corresponding xerogel. The mechanical relaxation spectrum shows the presence of a new water-induced relaxation, the water content dependence of the glass transition is measured by DSC, and the dielectric relaxation assesses the effect of water for the lower concentrations. Hydrophilic and hydrophobic monomeric units in the P(EA-*co*-HEA) network are able to aggregate to form two separated (nano)phases in the presence of water due to hydrophobic interaction. Phase separation takes place when the water content of the sample is higher than a critical value estimated as two water molecules per –OH group in the copolymer chain. The existence of the hydrophobic domains is detected by their glass transition being nearly independent on the water content of the sample. Phase separation is also clearly revealed by phase angle measurements in AFM experiments.

1. Introduction

The so-called hydrophobic interaction describes the aggregation of hydrophobic groups in the presence of water to minimize their exposure to water, and gives rise to weak intra- and inter-molecular interactions and the organisation of macromolecular assemblies. The interaction is theoretically well-understood when dealing with the properties of dilute solutions of apolar molecules in liquid water but it remains poorly understood when conformations of macromolecules and protein folding are concerned [1,2]. The existence of this kind of interaction is a consequence of the difficulties in the maintenance of the water hydrogen bond network around the hydrophobic assemblies. It is known that each water molecule can participate in four hydrogen bonds, sharing its two hydrogen atoms with two neighbouring water molecules and sharing two further hydrogen atoms associated with two other neighbours. Ice is a tetrahedrally ordered array, and liquid water a disordered network, of such hydrogen-bonded molecules [3]. The maintenance of this network has to do with length scales. If the exclusion volume of the hydrophobic molecule is small enough, its presence in water requires no breaking of hydrogen bonds. The situation is different in the case of large solutes in which it is impossible to maintain a complete hydrogen-bonding network with the surrounding liquid and a fraction of hydrogen-bonding possibilities are lost near the surface [4]. The tendency for hydrophobic particles to cluster in water has been explained in terms of the dependence of hydrophobic solvation on solute size: a cluster is formed when

* Corresponding author. Address: Center for Biomaterials, Universidad Politécnica de Valencia, 46022 Valencia, Spain. Tel.: +34 963877275; fax: +34 963877276.
E-mail address: masalsan@fis.upv.es (M. Salmerón Sánchez).

0014-3057/$ - see front matter © 2008 Elsevier Ltd. All rights reserved.
doi:10.1016/j.eurpolymj.2008.04.032

a sufficiently large volume to surface ratio is reached so that its solvation energy is lower than the overall solvation free energy of the individual components. However, the formation of a cluster from individual molecules implies the formation of a new surface and, as the nucleation theory shows, the formation of a critical nucleus is needed [5]. It has been shown that stable hydrophobic clusters in the presence of water are bigger than 1 nm [6].

Hydrophobic interactions have been invoked to account for conformational changes of single chains in polymer solutions that could not be explained by the conventional interaction between molecules [7]. The principles that hold for purely hydrophobic solutes apply to molecules containing some hydrophilic units, but additional entropic effects arise since both hydrophobic and hydrophilic units need to be accommodated [8]. When hydrophilic and hydrophobic groups are present in a molecule, the association of water molecules around the hydrophobic parts changes the polymer chains conformations from a random structure to a collapsed one [8–15]. Some copolymers bearing hydrophobic and hydrophilic groups when dissolved in water above a critical concentration tend to associate by inter-molecular hydrophobic interaction, generating a transient network via associations of the hydrophobic groups [16–20]. The distributions of monomeric units along the chain is an important factor to take into account when dealing with phase transitions in gels since it might lead to phase separation as a consequence of the molecular organization of the copolymer chain. Nevertheless, even in the case of a random copolymer, nanophase segregation could take place as a consequence of intra-chains associations. If the system investigated consisted of well-defined phases of hydrophilic and hydrophobic groups (such as a block copolymer or a phase-separated interpenetrated polymer network [21]), each one of the phases would behave in the presence of water as if the other component were not present, i.e. water molecules would associate around the hydrophilic phase neglecting the presence of the second one. This is not the case in the P(EA-*co*-HEA) system: it is homogeneous at the nanometric scale in the dry state, i.e. there is no evidence of phase separation by dynamic techniques (dielectric/mechanical spectroscopy).

For many applications hydrophilic–hydrophobic polymer networks are better than linear macromolecules and there is little information about the solvent-induced conformational changes in these kinds of topologically constrained systems. The conformational behaviour of cross-linked poly(alkylmethyldiallylammonium bromides) was investigated by fluorescence probing [20]. We have recently investigated poly(ethyl acrylate-*co*-hydroxyethyl acrylate), P(EA-*co*-HEA), networks swollen in benzene by DSC and the existence of conformational changes induced by the presence of the solvent was shown [21]. In this work, the conformational changes in a P(EA-*co*-HEA) network induced by the presence of water are investigated by different experimental techniques, and compared with the corresponding xerogels. The mechanical relaxation spectrum suggests the presence of a new water-induced relaxation. The phase diagram of the system shows how the effect of the hydrophobic aggregation modifies the glass transition temperature dependence of the system when compared to the case of homogeneously distributed polymer/water systems. The dielectric relaxation reveals the effect of water molecules for lower water contents. Finally, atomic force microscopy allows the direct visualisation of the water-induced formation of the aggregates.

2. Experimental

2.1. Materials

Monomers from Aldrich 99% pure were used without further purification. Copolymer networks were polymerized from the mixture of the ethyl acrylate, EA, and hydroxy ethylacrylate, HEA, co-monomers in proportion 50:50 wt.% via ultraviolet light, at room temperature, using 2 wt.% ethyleneglycol dimethacrylate, EGDMA (Aldrich, 98% pure), as cross-linking agent and 0.13 wt.% benzoine (Scharlau 98% pure) as photoinitiator. The polymerization took place in a mould that consisted of two glass plates with a rubber spacer what allowed to prepare a polymer sheet approximately 1 mm thick. The low molecular weight substances remaining in the sample after polymerization were extracted with boiling ethanol for 24 h and then the sample was dried at 60 °C in vacuo to constant weight. The yield of the process was above 95%.

2.2. Differential scanning calorimetry

Samples for DSC were cut from the copolymer plate and immersed in water for different times to obtain different water contents, ranging from very low ones to equilibrium values and subsequently pressed into the DSC pans. DSC was performed in a Pyris 1 apparatus (PerkinElmer). Helium gas was let through the DSC cell with a flow rate of 20 ml/min. The temperature of the equipment was calibrated with water and indium. The melting heat of indium was used for calibrating the heat flow. The samples were subjected to a cooling scan from ambient temperature to −100 °C, followed by a heating scan from that temperature to 20 °C—both scans at a rate of 10 °C/min. The characteristic transition temperatures were calculated from the DSC thermograms. The temperature of the inflexion point of the thermogram was taken as the glass transition temperature, T_g, of the swollen polymer, whereas for the phase transition of water it was the temperature of the maximum of the large exothermal or endothermal peak the one that was taken. The water mass in the swollen gel was determined gravimetrically. The solvent content in the swollen gel is quantitatively given by the water weight fraction, w, the ratio of the weight of water in the gel to the total weight of the gel

$$w = \frac{m_{\text{water}}}{m_{\text{water}} + m_{\text{dry polymer}}} \quad (1)$$

where m_{water} is the mass of water sorbed in the gel and $m_{\text{dry polymer}}$ is the mass of the xerogel. The water sorbed by the polymer referred to the mass of the hydrophilic component in it, is given by the water weight fraction, w', the ratio of the weight of water in the gel to the mass of water plus the mass fraction of water sorbed by the PHEA phase in the swollen gel

$$w' = \frac{m_{water}}{m_{water} + m_{HEA}} \quad (2)$$

where m_{HEA} is the mass of HEA in the polymer gel.

2.3. Dynamic mechanical analysis

Samples for dynamic-mechanical analysis, DMA, were cut from the copolymer plate. A first one was measured dry. A second one was let to swell in an ambient of humid air with a relative humidity of 11.30% at 20 °C maintained by a saturated solution of lithium chloride, to obtain very low water content; the third one was swollen to equilibrium by immersion in liquid water. A Seiko DMS 210 dynamic-mechanical analyser was used to perform dynamic-mechanical spectroscopy (DMS) at 1 Hz. The temperature dependence of storage modulus (E'), loss modulus (E'') and loss tangent (tan δ) was measured from −50 to 25 °C at a heating rate of 1 K/min.

2.4. Dielectric relaxation spectroscopy

Samples for Dielectric Relaxation Spectroscopy, DRS, were cut from the copolymer plate in the form of discs. Three of them were swollen in humid air atmospheres whose relative humidity, r.h. was controlled with different saturated salt solutions to obtain different low water contents, namely, lithium chloride (r.h. 11.30%), magnesium nitrate (r.h. 54.38%) and potassium sulphate (r.h. 97.59%). The forth one was dry. The DRS experiments were performed using an impedance analyzer Alpha-S. The temperature control was assured by the Quatro Cryosystem from Novocontrol GmbH. Samples were placed between two gold plated electrodes (diameter 20 mm) of a parallel-plate capacitor. The sample cell was mounted on a cryostat (BDS 1100) connected to a liquid nitrogen Dewar. In these experiments, the complex dielectric permittivity was determined as a function of frequency (10^{-1}–10^{7} Hz) in a temperature range between −50 °C and 50 °C.

2.5. Atomic force microscopy

Samples for Atomic Force Microscopy, AFM, were cut from the copolymer plate in the form of discs, dried in vacuo and measured in a NanoScope III from Digital Instruments operating in the tapping mode in air. Si-cantilevers were used with force constant of 42 N/m and resonance frequency of 290 kHz. The phase signal was set to zero at the resonance frequency of the tip. The tapping frequency was slightly lower than the resonance one. The same sample was swollen to equilibrium and then measured in tapping mode covered by a drop of liquid water. A Si-cantilever with constant force of 0.58 N/m was used for the AFM in the liquid mode.

3. Results

The glass transition of the hydrated samples is clearly shown in the DSC cooling scans (Figs. 1a and 1b). The glass transition temperature T_g shifts with increasing water content first towards lower temperatures until a water content of $w = 0.016$; it then increases, and the glass transition temperature of the sample with $w = 0.031$ is nearly the same as in the dry sample. For higher water contents T_g decreases with increasing water content very slightly, the difference between the T_g of the sample swollen in immersion in liquid water (the experimental point with the highest water content) and that of the dry sample is only 7 °C (Fig. 2). The same behaviour is shown in the heating scans for low water contents (below 0.031).

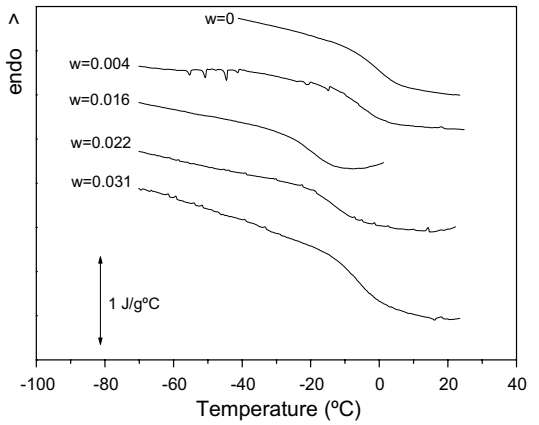

Fig. 1a. DSC cooling thermograms at 10 °C/min of samples with different water contents shown on each curve.

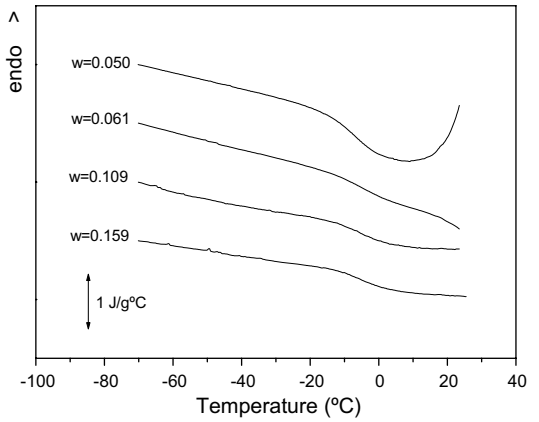

Fig. 1b. DSC cooling thermograms at 10 °C/min of samples with different water contents shown on each curve.

The cooling scans performed with samples containing higher water contents are analogous to that shown in Fig. 1 for $w = 0.031$. Fig. 3 shows the DSC curves corresponding to the sample swollen to equilibrium immersed in liquid water, $w = 0.159$. It is worth noting that no water crystallization takes place on cooling. Nevertheless, on subsequent heating of samples with water contents above $w = 0.031$ the thermogram shows some indications of water crystallization. No clear exothermic peak is shown, because of the superposition of a broad exotherm with the glass transition of the polymer phase. Nonetheless a small melting peak below 0 °C, whose phenomenology agrees with that water crystallized in equilibrium with the gel, indicates

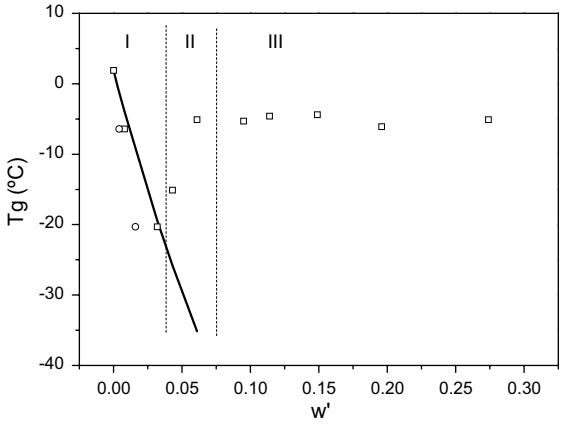

Fig. 2. Glass transition temperature as a function of the water content referred to the hydrophilic component, w' (Eq. (2)). The solid line represents the prediction of the Couchman–Karasz equation for the polymer/water homogeneous mixtures. Open symbols represent the glass transition temperature as a function of the water content, w, for samples with $w = 0.004$ and 0.016. Three qualitatively different areas are found: (I) plasticization of the hydrophilic domains in the copolymer, (II) abrupt change in the glass transition dependence as a consequence of the hydrophobic interaction, (III) glass transition of the hydrophobic domains.

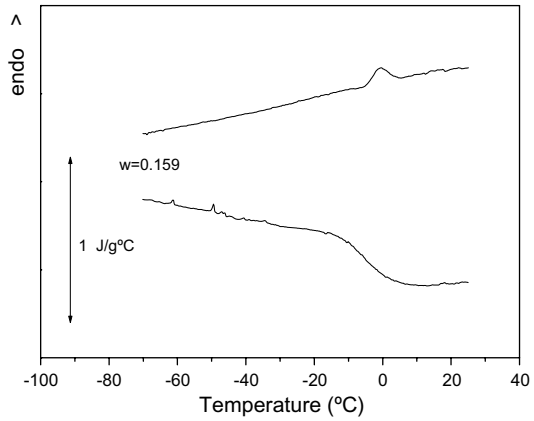

Fig. 3. DSC cooling (down) and heating (up) thermograms of a sample with the equilibrium water content in equilibrium in immersion in liquid water $w = 0.159$.

that a small amount of the absorbed water is in fact crystallized on heating [27].

Plasticization of the polymer network for low water contents is also clearly depicted in the dielectric results. Only some characteristic results DRS results will be shown. Fig. 4 shows the temperature dependence of imaginary component of the dielectric permittivity measured at 100 Hz. The peak in ε'' is characteristic of the main or α dielectric relaxation, related to the co-operative conformational rearrangements of the chains that constitute the polymer network. For low water contents, up to $w = 0.013$, a maximum in ε'' appears clearly, although its high temperature side is affected by the draught current (dc) conductivity contribution, leading to a continuous increase of ε'' with increasing temperature. As the water contents increases the contribution of the dc conductivity is more important and, in fact, in the samples with $w = 0.107$ or higher the dipolar peak cannot be distinguished. The plasticization of the polymer network by the water molecules produces the shift of the α relaxation towards lower temperatures. It is worth noting that in dielectric relaxation the water content interval that can be analysed only covers the lowest water contents and the increase of the glass transition observed by DSC from $w = 0.016$ up cannot be observed in DRS.

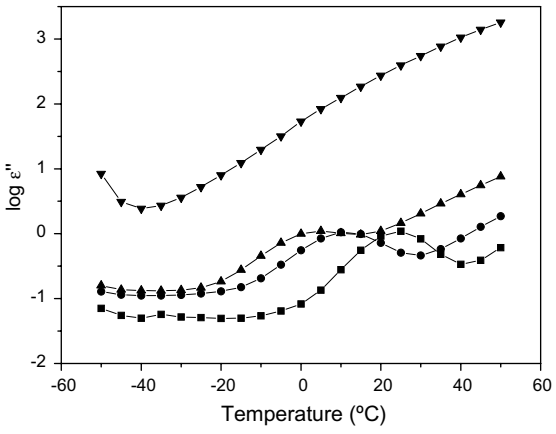

Fig. 4. Imaginary component of the dielectric permittivity of the dry sample (■) and samples with different water contents $w = 0.007$ (●), $w = 0.013$ (▲) and $w = 0.107$ (▼).

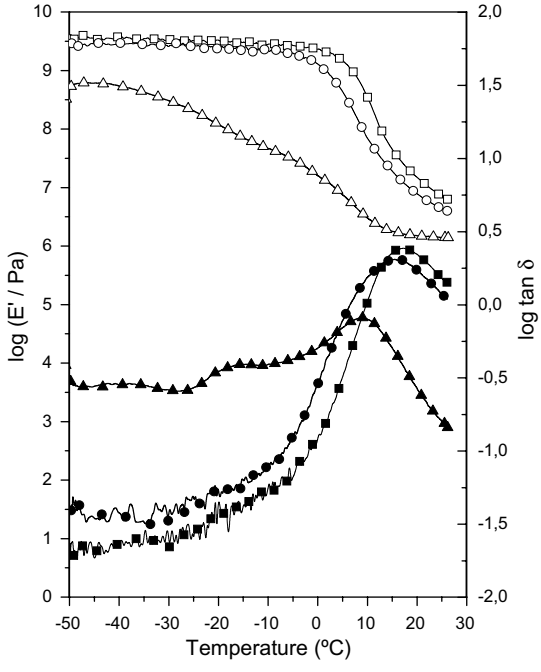

Fig. 5. Temperature dependence of the elastic modulus (open symbols) and the loss tangent (full symbols) of the dry sample (■), a sample with a water content $w = 0.007$ (●), and the sample swollen in equilibrium in immersion in liquid water $w = 0.159$ (▲).

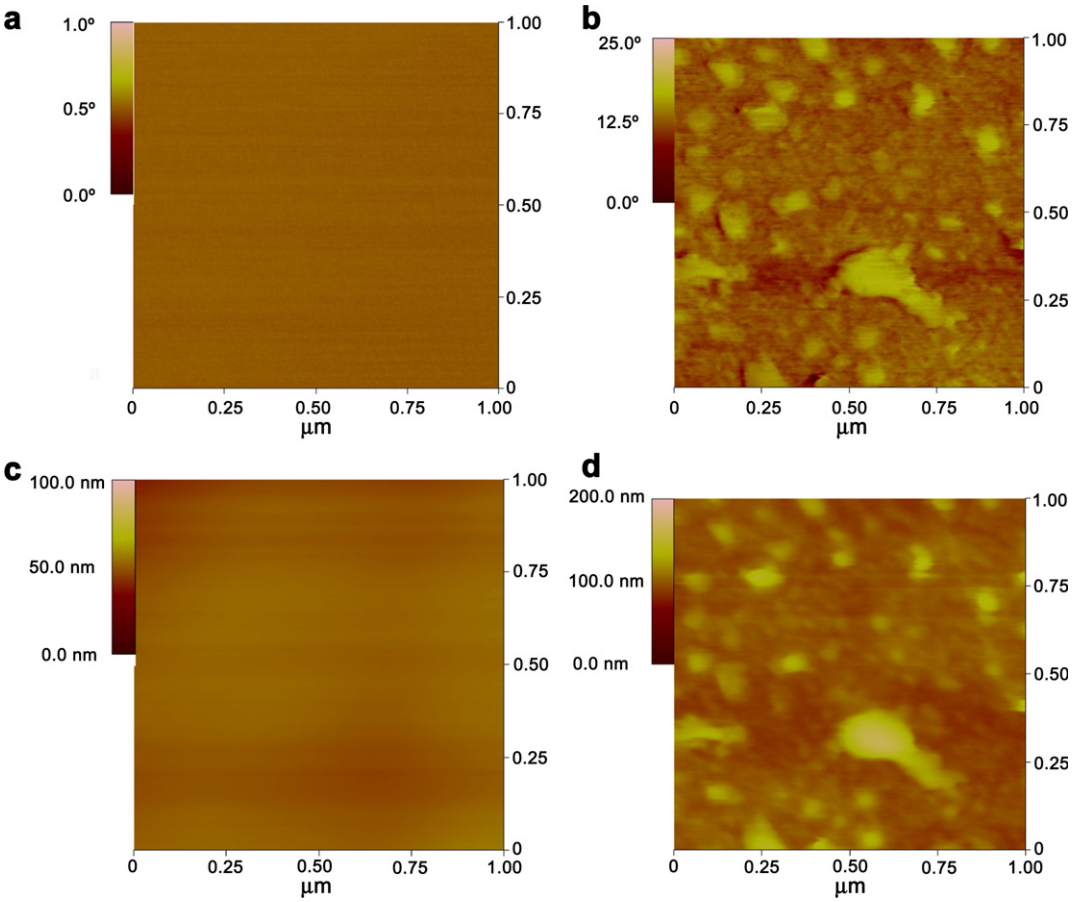

Fig. 6. AFM phase image, (a) and (b), and topography, (c) and (d), recorded in tapping mode of the dry copolymer xerogel, (a) and (c), and the swollen networks, (b) and (d), scanning a 1 μm × 500 × 500 1 μm area.

In the dynamic-mechanical analyser used in this work the sample is exposed to the cell atmosphere and the control of the water content of the sample is not as precise as in the DSC experiments, where the sample is encapsulated in sealed pans, or in the dielectric experiments, where the sample is between the cell electrodes. Only the dry sample, a sample with the maximum water content and an intermediate composition were used in these experiments. As shown in Fig. 5 the temperature of the maximum of the loss tangent is lower in the swollen networks than in the xerogel, but the maximum difference is only around 10 °C, similar to what found in DSC experiments. The main feature found in the dynamic-mechanical experiments is the presence of a second peak appearing in the loss tangent plot of the sample with $w = 0.159$ around −17 °C. This peak will be discussed in the next section as a consequence of the phase separation process in the sample due to the presence of water.

AFM experiments were performed on the dry sample, i.e. the xerogel, in the tapping mode in air atmosphere, and in tapping mode in the swollen sample previously equilibrated in liquid water and with the tip immersed in a drop of water deposited on the sample. The picture of the topography and phase angle clearly indicates that the surface of the xerogel is completely homogeneous (Fig. 6a and c). However, a pattern in which domains of hundred of nanometers of different viscoelastic properties alternate is clearly revealed when the sample is swollen (Fig. 6b and d).

4. Discussion

Copolymerization theory allows estimating, via the terminal model, the composition of the copolymer chain once the polymerization process is finished [22,23]. The monomer molar fraction F_i in the copolymer in terms of the monomer molar fraction in the reaction mixture f_i and the reactivity ratios r_i turns out to be

$$\frac{F_1}{F_2} = \frac{f_1(f_1 r_1 + f_2)}{f_2(f_2 r_2 + f_1)} \tag{3}$$

Reactivity ratios are 0.5 and 0.97 for EA and HEA, respectively, [24]. This difference has an immediate consequence. HEA radicals have a higher tendency to react with HEA monomers than with the EA ones. On the other hand, the lower EA reactivity ratio means that this monomer has a higher affinity towards HEA monomers than towards the EA ones. The composition predicted by the terminal model, Eq. (2), is shown in Fig. 7.

The theoretical prediction lies below the straight line that gives the random composition of the copolymer chain

(that is, the final copolymer keeping the same proportion of the two components present in the original reaction mixture).

In the copolymer network prepared from a 50:50 mixture of monomers, the amount of EA moieties in the copolymer chain is slightly lower than in the original mixture, what results in a network formed by copolymer chains where both EA and HEA are not randomly distributed, but where small blocks of HEA are preferentially present. However, the glass transition and the main dielectric and dynamic-mechanical relaxations of the xerogel show no indications of phase separation, i.e. spatial composition fluctuations with unimodal distribution. The length of cooperativity at the glass transition has been evaluated in amorphous polymers to be in the order of a few nanometers. This determines an order of magnitude for the size domains of a phase-separated system to present the glass transition of the individual phases. Although the polar (hydrophilic) groups along the chains are not randomly distributed, there is no sign of aggregation of polar or non-polar groups with dimensions sufficient to produce independent glass transitions in the xerogel.

In the first stages of absorption, until $w = 0.016$, the glass transition shifts to lower temperatures as corresponds to the homogeneous mixing of copolymer chains and water. To emphasize this feature the prediction of the Couchman–Karasz equation [25]

$$T_g = \frac{(1-w')\Delta c_{pCOP} T_{gCOP} + w'\Delta c_{p,water} T_{g,water}}{(1-w')\Delta c_{pCOP} + w'\Delta c_{p,water}} \quad (4)$$

for the glass transition temperature of the copolymer network is represented in Fig. 2. In this equation w' is the mass fraction of water per unit mass of HEA in the system, $T_{g,water} = 134\ K$ *and* $\Delta c_{p,water} = 1.94\ J\ g^{-1}\ K^{-1}$ have been taken from [26] while the values for the copolymer network $T_{g,COP} = 275.1$ K and $\Delta c_{p,COP} = 0.374\ J\ g^{-1}\ K^{-1}$ have been obtained experimentally in this work from the DSC curve corresponding to the xerogel (Fig. 1). It is important to remark that the line in Fig. 2 is not a fit to the experimental points but a prediction. The good agreement between the experimental points obtained from DSC measurements for low water contents and the theoretical curve can be interpreted in the sense that the initial amount of water which enters the system remains homogeneously mixed with the hydrophilic units of the copolymer chains in the network (region I in Fig. 2). The maximum amount of water in this regime is quite small, $w = 0.016$, and corresponds only to one water molecule per five –OH groups in the polymer chain.

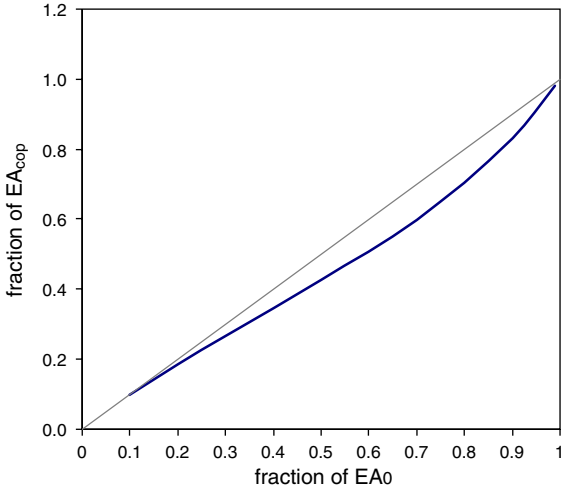

Fig. 7. Molar fraction of *EA* units in the copolymer as predicted by the terminal model (fraction of EA_{cop}) as a function of the molar fraction of *EA* monomers in the reacting mixture (fraction of EA_0). The straight line gives the composition of a random copolymer where the fraction of monomers of the original mixture is kept also in the polymerized material.

Exceeding this modest amount of water ($w = 0.016$) a rapid increase of the glass transition temperature is observed in the polymer network with respect to that expected for the homogeneous mixture of water molecules and polymer chains (region II in Fig. 2). The influence of the hydrophobic interaction on the glass transition temperature has been accounted for quantitatively for polymer networks with a hydrophilic and a hydrophobic component using the Kwei equation [21,27–30]. Nevertheless, the sharp increase of the glass transition in this case in a narrow range of water contents cannot be explained by the mere contribution of the interaction between hydrophobic monomer units in a homogeneous system. Rather, the behaviour shown is explained by phase separation between a hydrophobic non-plasticized phase and water-containing hydrophilic phase, leading to the formation of polymer (nano) aggregates in the copolymer chains. The experimental T_g depicted in Fig. 2 have been assigned to three qualitatively different regions: I describes the initial plasticization of the copolymer as a consequence of the first water molecules that enter the system. The initial accommodation of water into the system already conveys some conformational rearrangements leading to the incorporation of water preferentially next to the hydrophilic segments, as it is confirmed by the fact that experimental points fit to Couchman–Karasz equation when are plotted against w' instead of w. Region II is considered to be a consequence of a transition regime: further incorporation of water into the system gives rise to the so-called hydrophobic interaction leading to a process of nanophase separation which increases the glass transition temperature of the copolymer. Finally, region III describes the system for high water contents and the experimentally measured T_g is ascribed to the vitrification of the hydrophobic (nano) aggregates as it will be discussed in the following.

The organization of the hydrophobic and hydrophilic groups in these aggregates (region III in Fig. 2) must be rather imperfect due to the lack of regularity along the copolymer chains (as obtained from the interpretation of the terminal model, Fig. 7) and the presence of cross-links. Nevertheless the number of hydrophilic groups included in the hydrophobic domains is low enough to force that the core of the aggregates contain no water molecules, or at least, less water than the average. Further increase in the water uptake (from 0.05 on) reduces the observed glass transition temperature very slightly (Fig. 2), what means first that the glass transition depicted in the experimental thermograms for these water contents must be ascribed to the domains rich in the hydrophobic units of the copolymer and secondly that water molecules are accumulated

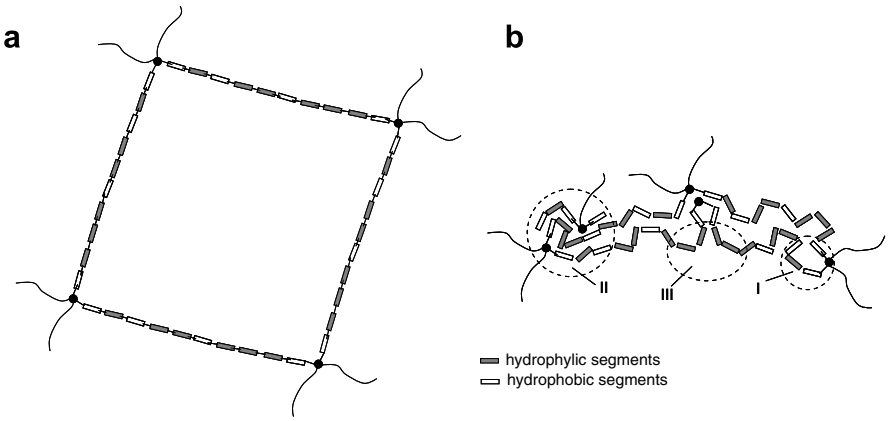

Fig. 8. Sketch of the molecular situation. (a) Ideal network compatible with the experimental results (absence of any kind of phase separation) and the prediction of the terminal model. The chain of the copolymer consists of hydrophilic units in which some hydrophobic segments alternate. It must be taken into account that in a polymer network the chains are not stretched but similar to random walks and entangled. Besides, for random cross-linking they are not of uniform length. (b) Water-induced organization of hydrophilic and hydrophobic aggregates. Domain I represents a hydrophobic aggregate. Domain II represents a hydrophobic aggregate with some hydrophilic segments trapped inside. Domain III represents a hydrophilic aggregate linked to hydrophobic segments unable to participate in conformational motions as a pure domain.

outside them, i.e. these organized domains are not plasticized by the presence of water in the copolymer network. It is worth noting that the fact that the glass transition of these hydrophobic domains can be detected by DSC proves that their size must be at least in the order of magnitude of the length of cooperativity at the glass transition temperature (approx. 10 nm) [34]. On the other hand, no glass transition of the hydrated domains can be detected by DSC, as shown in the cooling scan of Fig. 3, for the sample with the highest water content. In this sample the water content is around two water molecules per hydroxyl group. In the case of a pure PHEA network cross-linked with 2 wt.% EGDMA the amount of water absorbed in equilibrium by the sample immersed in liquid water are around ten molecules per –OH group [31]. In the case of the copolymer network of this work, the presence of the hydrophobic aggregates limits the expansion capacity of the network and, on the other hand, a number of hydroxyl groups must be trapped within the hydrophobic phase and thus being inaccessible by the water molecules. One can argue that the mobility in the hydrophilic phase does not allow the co-operative motions needed to produce the glass transition. The glass transition of the hydrophobic phase takes place at temperatures around that of the dry network (approx. −15 °C) [35]. This means that at lower temperatures (in the temperature interval in which the glass transition of the plasticized hydrophilic network would be expected to take place) the chain segments that pertain to the hydrophilic phase –that is swollen with water– are bonded to the glassy hydrophobic parts of the polymer network. The situation is somehow similar to that of the amorphous intraspherulitic phase of a semicrystalline polymer in which the mobility of the amorphous chains is strongly restricted by the presence of the crystallites [32,33]. This lack of mobility can explain the difficulty of the crystallization of water on cooling as well. Nevertheless some indication of the molecular rearrangements in this phase can be seen from the dynamic-mechanical experiments (Fig. 6), by the peak appearing in the loss tangent around −17 °C and the gradual decrease of the elastic modulus in the temperature interval between −30 and 20 °C. Note that no secondary relaxation appears in this temperature interval in pure PHEA hydrogels [36].

The phase separation induced by the presence of the solvent is clearly observed in the AFM pictures. Fig. 6 shows the area scanned on the same sample before (a–c) and after (b–d) water immersion. The homogeneity of the copolymer in the xerogel state is verified in the phase image (note the low scale for the phase angle). The bright aggregates in the phase images are identified with the hydrophobic domains whose size is large enough to account for an additional relaxation and glass transition in DSC. The formation of the aggregates has an effect also on the topography signal in AFM. Likewise, the topography picture for the xerogel is quite uniform up to approx. 100 nm and the presence of water induces the formation of aggregates that stick out the surface approx. 80–100 nm. It must be remarked here that AFM provides information on nanostructure formation on the surface of the samples swollen in water. However, it does not provide complete information about nanophase separation in the bulk. Such information could be obtained by, e.g., small-angle neutron scattering.

The molecular weight between cross-links can be estimated by the affine model in rubber elasticity theory [37]

$$\bar{M}_c = \frac{3\rho RT}{E} \tag{5}$$

where ρ is the density of the network, R the gas constant, T the temperature in the rubber state and E the Young elastic modulus. According to the data in Fig. 5, the molecular weight between cross-links in the dry network results approx. 1500 g/mol. Segregation beyond the size of the network requires a larger distortion of the network, and the length scale of the strand corresponding to $M_c \approx 1500$ g/mol is of the order of 10 nm, i.e. much smaller than the surface domain detected by AFM (100 nm). Thus, the network must be quite heterogeneous as a consequence

of the polymerization kinetics which results in a much scarcer network near the surface. Besides, rubber elasticity allows one to calculate the modulus of the swollen network E_w from the single knowledge of the modulus of the xerogel E and the volume fraction of solvent in the gel ϕ_1 [38],

$$E_w = (1 - \phi_1)^{\frac{1}{3}} E \quad (6)$$

Taking into account the equilibrium water content of the gel swollen in liquid water ($w = 0.159$), Eq. (5) predicts the modulus of the swollen network to be $E_w = 5.12$ MPa, much higher than the experimental value obtained from Fig. 3 $E_{exp} = 1.38$ MPa. The difference must be ascribed to the non-uniform distribution of water within the sample, i.e. to the formation of aggregates with more water than the average that lead to a poorer mechanical behaviour.

5. Conclusions

Hydrophilic and hydrophobic monomeric units in the poly(ethyl acrylate-*co*-hydroxyethyl acrylate) copolymer network are able to organize to form two separated phases in presence of water due to hydrophobic interaction. Phase separation takes place when the water content of the sample is higher than a critical value estimated in two water molecules per –OH group in the polymer chain. The existence of the hydrophobic domains is detected by their glass transition nearly independent on the water content of the sample. Phase separation is also clearly revealed by phase angle measurements in AFM experiments.

Even though is difficult to sketch the molecular situation of this system, Fig. 8a represents an ideal network compatible with the experimental results (absence of any kind of phase separation) and the prediction of the terminal model. The length of either hydrophilic or hydrophobic segments is not long enough as to behave as phase-separated system and, consequently, the dynamic response of the system does not consist of two independent processes at the temperatures of the corresponding pure components. Besides, the composition of the copolymer chain is in agreement with the terminal model. On the other hand, Fig. 8b is an attempt to sketch the organization of the hydrophilic and hydrophobic units in the presence of water. Three kind of aggregates are inferred: I represents pure hydrophobic domains; II accounts for hydrophobic domains with entrapped hydrophilic units where water cannot access and, consequently are not able to plasticize; III represents hydrophilic domains linked to hydrophobic segments that are not able to participate in conformations at the temperature of the corresponding pure hydrophilic component due to the steric hindrance of the hydrophobic domain that is a glass at those temperatures.

Acknowledgements

Authors acknowledge the support of the Spanish Ministry of Science and Education through the MAT2006-08120 (including the FEDER financial support). AFM was conducted by the authors in the Microscopy Service of the Universidad Politécnica de Valencia, whose advice was greatly appreciated.

References

[1] Pratt LR, Chandler D. Theory of the hydrophobic effect. J Chem Phys 1977;67:3683–704.
[2] Wiggins PM. Hydrophobic hydration, hydrophobic forces and protein folding. Physica A 1997;238:113–28.
[3] Chandler D. Hydrophobicity: Two faces of water. Nature 2002;417:491.
[4] Chandler D. Interfaces and the driving force of hydrophobic assembly. Nature 2005;437:640–7.
[5] Debenedetti PG. In metastable liquids. Princeton, NJ: Princeton University Press; 1996.
[6] Raschke TM, Tsai J, Levitt M. Quantification of the hydrophobic interaction by simulations of the aggregation of small hydrophobic solutes in water. Proc Natl Acad Sci USA 2001;98:5965–9.
[7] Ben-Naim A. In hydrophobic interactions. New York: Plenum Press; 1980.
[8] Grinberg NV, Dubovik AS, Grinberg VY, Kuznetsov DV, Makhaeva EE, Grosberg AY, et al. Studies of the thermal volume transition of poly(*N*-isopropylacrylamide) hydrogels by high-sensitivity differential scanning microcalorimetry. 1. Dynamic effects. Macromolecules 1999;32:1471–5.
[9] Tokuhiro T, Amiya T, Mamada A, Tanaka T. NMR study of poly(*N*-isopropylacrylamide) gels near phase transition. Macromolecules 1991;24:2936–43.
[10] Shibayama M, Mizutani S, Nomura S. Thermal properties of copolymer gels containing *N*-isopropylacrylamide. Macromolecules 1996;29:2019–24.
[11] Shibayama M, Morimoto M, Nomura S. Phase separation induced mechanical transition of poly(*N*-isopropylacrylamide)/water isochore gels. Macromolecules 1994;27:5060–6.
[12] Shibayama M, Suetoh Y, Nomura S. Structure relaxation of hydrophobically aggregated poly(*N*-isopropylacrylamide) in water. Macromolecules 1996;29:6966–8.
[13] Suetoh Y, Shibayama M. Effects of non-uniform solvation on thermal response in poly(*N*-isopropylacrylamide) gels. Polymer 2000;41:505–10.
[14] Wu C. A comparison between the 'coil-to-globule' transition of linear chains and the "volume phase transition" of spherical microgels. Polymer 1998;39:4609–19.
[15] Tsunashima Y, Kawanishi H, Horii F. Reorganization of dynamic self-assemblies of cellulose diacetate in solution: dynamical critical-like fluctuations in the lower critical solution temperature system. Biomacromolecules 2002;3:1276–85.
[16] Zhang YX, Da AH. A fluorocarbon-containing hydrophobically associating polymer. J Polym Sci Polym Part C. Polym Lett 1990;28:213–8.
[17] Zhang YX, Da AH, Butler GB, Hogen-Esch TE. A fluorine-containing hydrophobically associating polymer I. Synthesis and solution properties of copolymers of acrylamide and fluorine-containing acrylates or methacrylates. J Polym Sci Part A 1992;30:1383–91.
[18] Xie X, Hogen-Esch TE. Copolymers of *N*,*N*-dimethylacrylamide and 2-(*N*-ethylperfluorooctanesulfonamido)ethyl acrylate in aqueous media and in bulk. Synthesis and properties. Macromolecules 1996;29:1734–45.
[19] Ng WK, Tam KC, Jenkins RD. Rheological properties of methacrylic acid/ethyl acrylate co-polymer: comparison between an unmodified and hydrophobically modified system. Polymer 2001;42:249–59.
[20] Wang GJ, Engberts JBFN. Fluorescence probing of the formation of hydrophobic domains by cross-linked poly(alkylmethyldiallylammonium bromides) in aqueous solution. Recl Trav Chim Pays-Bas 1994;113:390–3.
[21] Salmerón Sánchez M, Monleón Pradas M, Gómez Ribelles JL. Thermal transitions of benzene in copolymers and interpenetrating polymer networks based on hydrophilic and hydrophobic components. J Polym Sci Part B Polym Phys 2003;41:1713–21.
[22] Mayo FR, Lewis FM. Copolymerization I. A basis for comparing the behavior of monomers in copolymerization; the copolymerization of styrene and methyl methacrylate. J Am Chem Soc 1944;66:1594–601.
[23] Alfrey T, Goldfinger G. The mechanism of copolymerization. J Chem Phys 1944;12:205–9.
[24] Brandrup J, Immergut EH. In polymer handbook. 3rd ed. New York: John Wiley & Sons; 1989. Chapter II.
[25] Couchman PR. Compositional variation of glass-transition temperatures. 2. Application of the thermodynamic theory to compatible polymer blends. Macromolecules 1978;11:1156–61.
[26] Johari GP, Hallbrucker A, Mayer E. The glass–liquid transition of hyperquenched water. Nature 1987;330:552–3.

[27] Salmerón Sánchez M, Gallego Ferrer G, Monleón Pradas M, Gómez Ribelles JL. Influence of the hydrophobic phase on the thermal transitions of water sorbed in a polymer hydrogel based on interpenetration of a hydrophilic and a hydrophobic network. Macromolecules 2003;36:860–6.
[28] Kwei TK. The effect of hydrogen-bonding on the glass-transition temperatures of polymer mixtures. J Polym Sci Polym Part C. Polym Lett 1984;22:307–13.
[29] Kwei TK, Pearce EM, Pennacchia JR, Charton M. Correlation between the glass transition temperatures of polymer mixtures and intermolecular force parameters. Macromolecules 1987;20: 1174–6.
[30] Krakovský I, Salmerón Sánchez M. Thermal transitions and structure of epoxy networks based on α,ω-diamino terminated poly(propylene oxide)-block-poly(ethylene oxide)-block-poly(propylene oxide) swollen in water. J Polym Sci Part B Polym Phys 2005;43:699–708.
[31] Pérez Olmedilla M, Garcia-Giralt N, Monleón Pradas M, Benito Ruiz P, Gómez Ribelles JL, Cáceres Palou E, et al. Response of human chondrocytes to a non-uniform distribution of hydrophilic domains on poly (ethyl acrylate-*co*-hydroxyethyl methacrylate) copolymers. Biomaterials 2006;27:1003–12.
[32] Alves NM, Mano JF, Balaguer E, Meseguer Dueñas JM, Gómez Ribelles JL. Glass transition and structural relaxation in semi-crystalline poly(ethylene terephthalate): a DSC study. Polymer 2002;43:4111–22.
[33] Wang Y, Gómez Ribelles JL, Salmerón Sánchez M, Mano JF. Morphological contributions to glass transition in poly(L-lactic acid). Macromolecules 2005;38:4712–8.
[34] Donth E. In relaxation and thermodynamics in polymers, glass transition. Berlin: Akademie Verlag; 1992.
[35] Salmerón Sánchez M, Monleón Pradas M, Gómez Ribelles JL. Thermal transitions of benzene in a poly(ethyl acrylate) network. J Non-Cryst Solids 2002;307:750–7.
[36] Monleón Pradas M, Gómez Ribelles JL, Serrano Aroca A, Gallego Ferrer G, Suay Antón J, Pissis P. Interaction between water and polymer chains in poly(hydroxyethyl acrylate) hydrogels. Colloid Polym Sci 2001;279:323–30.
[37] Flory PJ. In principles of polymer chemistry. Ithaca, NY: Cornell University Press; 1966.
[38] Siegfried DC, Thomas DA, Sperling LH. A reexamination of polystyrene/polystyrene homo interpenetrating polymer networks: aspects of relative network continuity and internetwork coupling. Macromolecules 1979;12:586–9.